Supplemental Information for:
RH-dependent organic aerosol thermodynamics via an efficient reduced-complexity framework

Kyle Gorkowski[1], Thomas C. Preston[1, 2], and Andreas Zuend[1]

[1]Department of Atmospheric and Oceanic Sciences, McGill University, Montreal, Quebec, Canada
[2]Department of Chemistry, McGill University, Montreal, Quebec, Canada

Correspondence: Kyle Gorkowski (kyle.gorkowski@mcgill.ca), Andreas Zuend (andreas.zuend@mcgill.ca)

1 Overview

The supplemental information covers the BAT model equations and the approaches for the parameterizations of different functional group classes and phase separation treatments. These approaches include the O : C blending method developed for the transition regions between the three BAT model parameterization regions, the functional group translations approach to convert input parameters to OH-group equivalents, finding the $a_{w,\mathrm{sep}}$ point for the liquid–liquid transition from a organic-rich to a water-rich phase, and the density estimation method for organic compounds. The attached supplemental Microsoft® Excel workbook file contains all the coefficient values, the SOA model system's input properties, and all the data shown in the figures of the main text.

2 BAT model

2.1 BAT Equations

The explicit equations for our BAT model are listed below in Eqs. (S1) to (S11). To improve the clarity, we define $\mathrm{O:C} \equiv \vartheta$, where O : C refers to the O : C of an organic component ("org") or the average O : C of a mixture of organics. The determined coefficients are listed in Tables S1 & S2.

$$c_1 = a_{1,1}\ \exp(a_{1,2}\ \vartheta) + a_{1,3}\ \exp\left(a_{1,4}\ \frac{M_w}{M_{org}}\right) \tag{S1}$$

$$c_2 = a_{2,1}\ \exp(a_{2,2}\ \vartheta) + a_{2,3}\ \exp\left(a_{2,4}\ \frac{M_w}{M_{org}}\right) \tag{S2}$$

$$\phi_{org} = x_{org}\left(x_{org} + (1 - x_{org})\frac{\rho_{org}}{\rho_w}\frac{M_w}{M_{org}}\left[s_1(1+\vartheta)^{s_2}\right]\right)^{-1} \tag{S3}$$

$$G^E/RT = \phi_{org}(1-\phi_{org})\left[c_1 + c_2(1-2\phi_{org})\right] \tag{S4}$$

$$\frac{d(G^E/RT)}{dx_{org}} = \frac{d(G^E/RT)}{d\phi_{org}}\frac{d\phi_{org}}{dx_{org}} \tag{S5}$$

$$\frac{d\phi_{org}}{dx_{org}} = \left(\frac{\rho_{org}}{\rho_w}\frac{M_w}{M_{org}}\left[s_1(1+\vartheta)^{s_2}\right]\right)\left(\frac{\phi_{org}}{x_{org}}\right)^2 \tag{S6}$$

$$\frac{d(G^E/RT)}{dx_{org}} = \left\{(1-2\phi_{org})\left[c_1 + c_2(1-2\phi_{org})\right] - 2c_2\phi_{org}(1-\phi_{org})\right\}\frac{d\phi_{org}}{dx_{org}} \tag{S7}$$

$$\ln(\gamma_{org}) = (G^E/RT) + (1-x_{org})\frac{d(G^E/RT)}{dx_{org}} \tag{S8}$$

$$a_{org} = \gamma_{org}x_{org} \tag{S9}$$

$$\ln(\gamma_w) = (G^E/RT) - x_{org}\frac{d(G^E/RT)}{dx_{org}} \tag{S10}$$

$$a_w = \gamma_w(1-x_{org}) \tag{S11}$$

Here, the activity coefficients of organic and water, γ_{org} and γ_w, respectively, as well as the corresponding activities (a_{org}, a_w) are defined on mole fraction basis (i.e. γ_{org} = $\gamma_{org}^{(x)}$), each with the pure component as reference and standard states (where activity coefficients become unity). The output from the BAT calculation can also be used to calculate the Gibbs energy of mixing ($\Delta_{\mathrm{mix}}G$), since the non-ideal interactions are parameterized (i.e., the excess Gibbs energy of mixing: G^{E}). Note, for simplicity, we do not include standard state chemical potentials of water and the organic, which would add an additional linear component to the curve. This is deemed justified given the approximate nature of the miscibility gap treatment. We present this calculation below with $\Delta_{\mathrm{mix}}G$ being normalized by R, T, and the total sum of moles $n_t = n_w + n_{org}$ in the binary system.

$$\frac{\Delta_{\mathrm{mix}}G^{\mathrm{ideal}}}{RTn_t} = (1-x_{org})\ln(1-x_{org}) + x_{org}\ln(x_{org}) \tag{S12}$$

$$\frac{\Delta_{\mathrm{mix}}G}{RTn_t} = \frac{\Delta_{\mathrm{mix}}G^{\mathrm{ideal}}}{RTn_t} + \frac{G^E}{RTn_t} \tag{S13}$$

Table S1. Scaled volume coefficients of the fitted BAT model.

Region	O : C bounds	s_2	s_1
low O : C	$\mathrm{O:C} < 0.15$	-5.988895	6.940689
mid. O : C	$0.05 < \mathrm{O:C} < 0.1\vartheta_{\mathrm{ML}}$	-1.219164	4.742729
high O : C	$\vartheta_{\mathrm{ML}} < \mathrm{O:C}$	-0.078682	3.650860
misciblity line	$0.05 < \mathrm{O:C} < 0.45$	-1.237227	4.069905

Table S2. The eight power series coefficients ($a_{n,1-4}$; $n = 1, 2$) used in the hydroxyl-group-parameterized BAT model.

Region	$a_{1,1}$	$a_{2,1}$	$a_{1,2}$	$a_{2,2}$	$a_{1,3}$	$a_{2,3}$	$a_{1,4}$	$a_{2,4}$
low O : C	7.089476	-0.622678	-7.711860	-100.0	-38.859410	3.08E-09	-100.0	61.888120
mid. O : C	5.872214	-0.974049	-4.535007	-100.0	-5.129327	2.109751	-28.092320	-23.676830
high O : C	5.921550	-100.0	-2.528295	-100.0	-3.883017	1.353916	-7.898128	-11.601450
misciblity line	5.885109	-0.984901	-4.731250	-6.227207	-5.201652	2.320286	-30.822970	-25.840370

2.2 Limit of Miscibility Line

The limit of miscibility line is determined from an initial BAT model fitting involving the O : C region close to where the miscibility gap *vs.* complete miscibility transition occurs. The resulting O : C values defining the limit of miscibility line, ϑ_{ML}, as a function of organic molar mass, was determined as

$$\vartheta_{\mathrm{ML}} = \frac{0.205}{1 + \exp\left(26.6\left(\frac{M_w}{M_{org}} - 0.12\right)\right)^{0.843}} + 0.23. \tag{S14}$$

2.3 O : C Transition Region Blending

We used three different sets of fitted coefficients for the base BAT model representing hydroxyl functionality molecules. The split was based on the limit of complete miscibility of organics with water and further separated by O : C. A sigmoidal function was introduced to provide a smooth transition when traversing from one of the domains to the next in the 2-D parameter space (e.g., when O : C is increased gradually at a constant molar mass coordinate) – otherwise, spurious discontinuities would occur. The sigmoidal function provides a weighted map between the parameters from one domain to the next (over a short range in the boundary region). In effect, we are blending the different regions in the hydroxyl BAT model. Low to medium O : C region blending is listed first (Eqs. S15 to S22), where ϑ_{ML} is the ϑ value at the limit of miscibility line and b_1, b_2, and b_{ML} are the

Table S3. Coefficients used in the blending of the different BAT coefficient regions for a molecule with hydroxyl functionality.

Region Transition	b_1	b_2	b_{ML}
low to mid. O : C	79.2606902	6.04293E-02	0.1899745
mid. to high O : C	75.0159268	9.47111E-04	-

blending coefficients (Table S3).

$$\vartheta_b = \vartheta - \vartheta_{\mathrm{ML}} b_{\mathrm{ML}} \tag{S15}$$

$$\varpi_b = \frac{1}{1+\exp[-b_1(\vartheta_b - b_2)]} \tag{S16}$$

$$\vartheta_{b,norm} = \vartheta - 0.75\,\vartheta_{\mathrm{ML}}\,b_{\mathrm{ML}} \tag{S17}$$

$$\varpi_{norm} = \frac{1}{1+\exp(-b_1(\vartheta_{b,norm} - b_2))} \tag{S18}$$

$$\varpi_{mid} = \varpi_b / \varpi_{norm} \tag{S19}$$

$$\varpi_{low} = 1 - \varpi_{mid} \tag{S20}$$

$$G^E/RT\Big|_{blended} = \varpi_{low}\, G^E/RT\Big|_{low} + \varpi_{mid} G^E/RT\Big|_{mid} \tag{S21}$$

$$\frac{d(G^E/RT)}{dx_{org}}\Big|_{blended} = \varpi_{low}\,\frac{d(G^E/RT)}{dx_{org}}\Big|_{low} + \varpi_{mid}\,\frac{d(G^E/RT)}{dx_{org}}\Big|_{mid} \tag{S22}$$

Medium to high O : C region blending (Eqs. S23 to S27):

$$\vartheta_b = \vartheta - \vartheta_{\mathrm{ML}} \tag{S23}$$

$$\varpi_{high} = \frac{1}{1+\exp(-b_1(\vartheta_b - b_2))} \tag{S24}$$

$$\varpi_{mid} = 1 - \varpi_{high} \tag{S25}$$

$$G^E/RT\Big|_{blended} = \varpi_{high} G^E/RT\Big|_{high} + \varpi_{mid} G^E/RT\Big|_{mid} \tag{S26}$$

$$\frac{d(G^E/RT)}{dx_{org}}\Big|_{blended} = \varpi_{high}\frac{d(G^E/RT)}{dx_{org}}\Big|_{high} + \varpi_{mid}\frac{d(G^E/RT)}{dx_{org}}\Big|_{mid}. \tag{S27}$$

2.4 BAT Functional Group Translation

The translation approach concerns the conversion from different functional group classes to hydroxyl-equivalent input parameters for use with the default, hydroxyl-group-based BAT model. These translations are for the whole molecule, and not the individual functional groups. Thus, for multifunctional molecules, a distinct multifunctional translation must be derived,

Table S4. Functional group translation coefficients to convert a whole molecule to a hydroxyl-equivalent molecule for BAT model inputs.

t_n	Hydroxyl	Carboxyl	Hydroperoxide	Hydroperoxide SOA	PEG	Ketone	Ether	Ester
t_1	none	none	8.1716E-06	1.4902E-04	5.4477E-03	4.5343E-03	2.4434E-05	-1.293246
t_2	none	none	4.5318E-07	4.7363E-03	3.864336	6.4845E-04	1.5832E-04	1.0813E-03
t_3	none	none	0.966090	0.869058	-0.267168	0.138144	0.284974	1.240514
t_4	none	none	0.459433	0.564783	0.255487	0.352454	0.229339	0.405354

as we did for the SOA oxidation products. If that is not possible, then the most dominant and representative functionality should be chosen. The O : C conversion is described by Eq. S28 and the molar mass translation is described by Eq. S29. The corresponding coefficients for different oxygen-bearing functionalities of the whole molecule are listed in Table S4.

$$\vartheta_{eqv.\,\mathrm{OH}} = \frac{\vartheta}{1 + t_3 \exp(-t_1\,\vartheta)} \tag{S28}$$

$$M_{eqv.\,\mathrm{OH}} = \frac{M}{1 + t_4 \exp(-t_2\,M)} \tag{S29}$$

3 Water Activity Separation Point

In the case of a liquid–liquid equilibrium, the relative phase preferences are described by q_j^α, the fractional liquid–liquid partitioning of a component to phase α ($q_j^\alpha \leq 1.0$ in the two-liquid-phases case). Liquid–liquid phase separation in a binary water–organic system at RH $< 100\,\%$ is reduced to a point and manifests itself by a jump discontinuity. The liquid phase is either a water-poor (β) or water-rich (α) phase, with a sharp transition between these two possible states at a specific water activity ($q_j^\alpha = 1$ or 0). To approximate the location and a_w-width over which the liquid–liquid phase separation is prescribed to occur, we first determine a designated reference point, the so-called water activity separation point ($a_{w,\mathrm{sep}}$). Liquid–liquid phase separation connects two points on the Gibbs energy of mixing curve that have identical slopes and a tie-line that does not cross the Gibbs energy curve (Fig. S1a). This tie-line represents the connection between the two stable phase compositions at equilibrium. Prior to phase separation occurring, a mixture can enter the composition space past these two points, which will result in a metastable state and eventually an unstable state, which will lead to spontaneous, spinodal decomposition (if phase separation did not occur within the metastable region). The binary mixture can enter and remain in the metastable region, but the energy barrier for liquid–liquid phase separation is typically low at room temperature, such that phase separation is expected to occur when the water content is increased. In most cases we will be interested in a case of increasing or decreasing water mole fraction at approximately constant temperature, so our $a_{w,\mathrm{sep}}$ point in Fig. S1a will be p_2, which has a corresponding point p_5 near/within the metastable composition range. If we solved for the tie-lines at high precision and included the standard state chemical potentials of water and the organic, then points p_1 and p_2 would have identical activities. That however is not the case, but we still want to ensure identical water activities at $a_{w,\mathrm{sep}}$. We achieve this by finding p_2's corresponding point (p_5) which has the same water activity as the $a_{w,\mathrm{sep}}$ point, this ensures a realistic water-poor (β) to water-rich (α) transition.

Here, we explain how to identify (to good approximation) the two stable composition points in liquid–liquid equilibrium by only using the BAT-predicted activity curves (Fig. S1b). In a binary system, both component activities must be less than one and have monotonic behavior. Any regions that show non-monotonic behavior result in a phase separation range and are denoted by the dashed lines in Fig. S1b. By connecting the mole fraction extent of the organic and water activity-based (minimum) phase separation regions identified, we can construct the tie-line that connects the two stable phases over the full extent of phase separation. This tie-line is then used in our above description to find the $a_{w,\mathrm{sep}}$ point. We note that due to omitting a computationally costly Gibbs energy minimization (with further including standard chemical potentials), the identified miscibility gap is a (typically good) approximation of the true extent of phase separation.

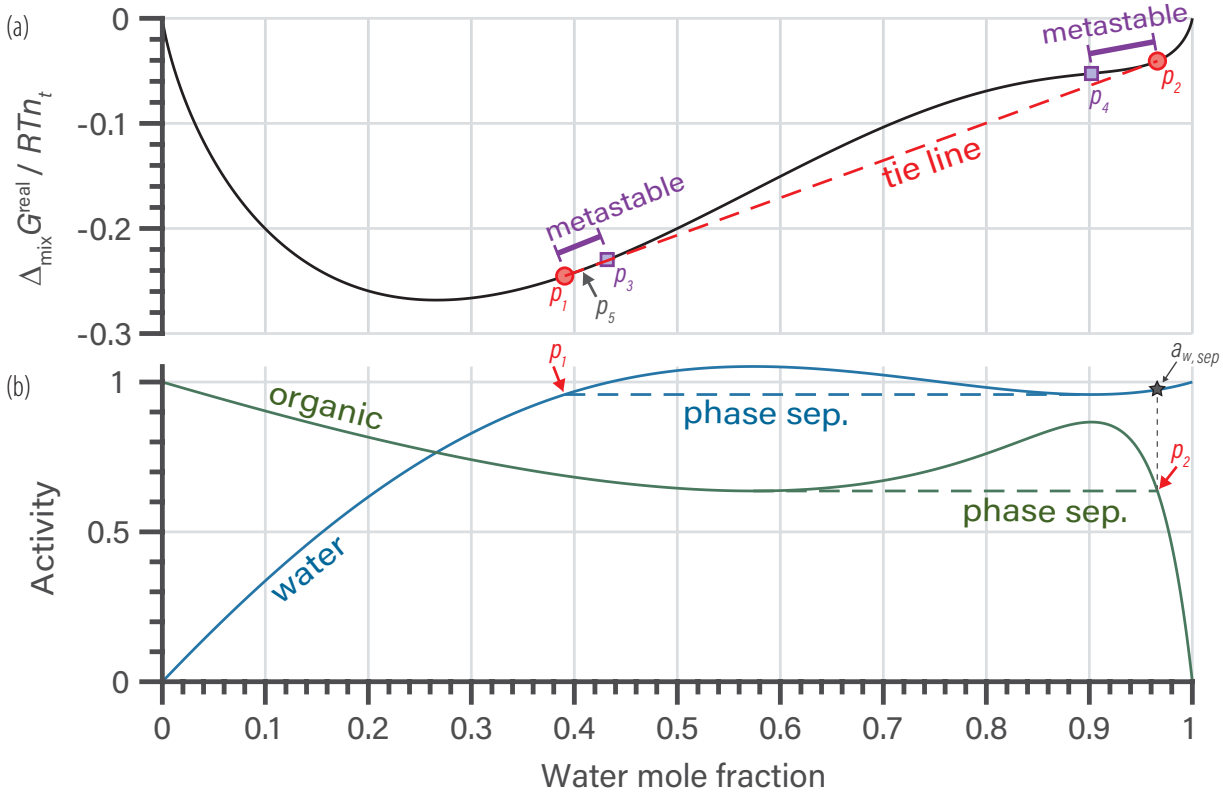

Figure S1. BAT simulation used to describe the identification of the $a_{w,\mathrm{sep}}$ point. The simulation uses an organic compound with hydroxyl functionalities, M_{org} of 100 g mol^{-1} and O : C of 0.225. The identified $a_{w,\mathrm{sep}}$ value is here 0.9741 (black star). (a) The normalized $\Delta_{\mathrm{mix}}G$ curve (black) with the tie-line in dashed red. The approximate stable phase-separation tie-line points and compositions are marked by p_1 and p_2, with the extent of the corresponding metastable regions denoted by p_3 and p_4. The end point in the metastable region at the same water activity as p_2 is marked by p_5. (b) The organic (green) and water (blue) mole-fraction-based activities for this binary system. The apparent minimum regions of phase separation required by each component are indicated by dashed lines. The approximate mole fraction extent of the actual phase separation region is identified by the extremes in composition, i.e. end points p_1 and p_2. The $a_{w,\mathrm{sep}}$ point is the water activity corresponding to the composition at p_2, indicated by a black star.

4 Organic Density Estimation

Organic density model from Girolami (1994), Eqs. (S34 to S37). If $\mathrm{H:C}$ is not known then we use $\mathrm{H:C} = 2 - \vartheta$.

$$M_C = 12.010\ \mathrm{g\,mol^{-1}} \tag{S30}$$

$$M_N = 14.006\ \mathrm{g\,mol^{-1}} \tag{S31}$$

$$M_O = 16.0\ \mathrm{g\,mol^{-1}} \tag{S32}$$

$$M_H = 1.008\ \mathrm{g\,mol^{-1}} \tag{S33}$$

$$n_c = \frac{M_{org}}{M_C + M_H\,\mathrm{H:C} + M_O\,\vartheta + M_H\,\mathrm{N:C}} \tag{S34}$$

$$\rho^* = \frac{M_{org}}{5 n_c (2 + \mathrm{H:C} + 2\,\vartheta + 2\,\mathrm{N:C})} \tag{S35}$$

$$\rho_{est.} = \rho^* (1 + \min(0.1\,n_c\,\vartheta + 0.1\,n_c\,\mathrm{N:C},\ 0.3)) \tag{S36}$$

$$\tag{S37}$$

5 SOA Mixtures

The model comparison focuses on the predictions of bulk liquid aerosol mass concentration, and we used the AIOMFAC-based equilibrium gas–particle partitioning predictions as a benchmark. The AIOMFAC-equil. calculations include consideration of liquid–liquid phase separation and consider relatively high-fidelity input, as the AIOMFAC model uses functional group information and accounts for non-ideal interactions among all species. In contrast, the VBS + BAT approach only includes non-ideal water $\leftrightarrow$ organic interactions (implicitly assuming ideal organic $\leftrightarrow$ organic mixing) and rather limited molecular structure information ($\mathrm{O:C}$ and M_{org}). The full extent of the percentage difference in organic aerosol mass between the VBS + BAT approach and AIOMFAC-equil. is shown in Fig. S2.

For our simulated aerosol systems, we use surrogate systems representing α-pinene SOA (Table S5) and isoprene SOA (Table S6) products based on predictions from the Master Chemical Mechanism, as was detailed in Zuend and Seinfeld (2012) and Chen et al. (2011), respectively. The α-pinene SOA system used here contains 10 organic species as surrogates of the SOA, and the isoprene SOA system is comprised of 21 organic surrogate species.

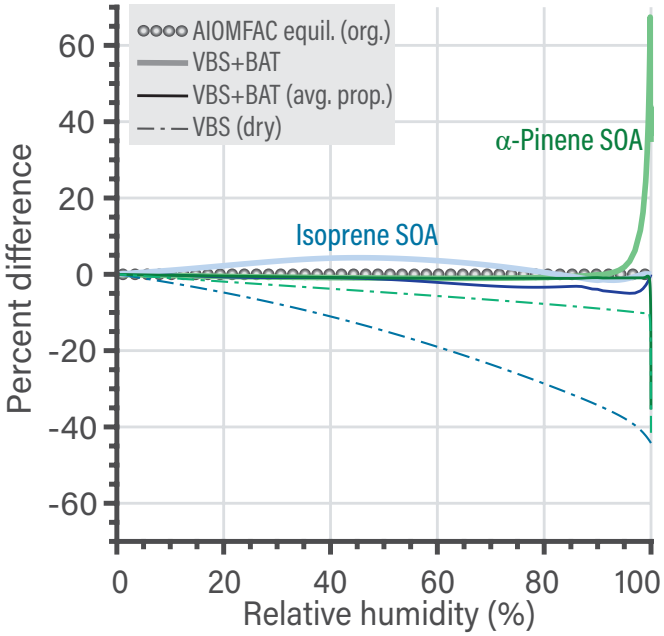

Figure S2. Percent difference in organic aerosol mass between the VBS + BAT approach and AIOMFAC-equil. as a function of equilibrium relative humidity for a bulk solution ($= a_w$) at 298.15 K. Simulations for isoprene SOA are shown in blue and those for α-pinene SOA in green. The benchmark AIOMFAC equilibrium predictions are shown for the salt-free cases (circles). The thick curves show the VBS + BAT prediction with different organic components, while the thin curve shows a simulation assuming an average molecule calculated from the dry mass, i.e., average O : C, H : C, M_{org}, and we kept the individual molecule's effective C^{sat}_{dry}. The thin dashed line shows the percent difference in the standard VBS simulation with no water uptake (dry).

Table S5: Properties of the α-pinene SOA organic mixture used.

Start of Table S5							
MCM Name	SMILES	BAT functionality	O : C	H : C	M_{org} ($\mathrm{g\,mol^{-1}}$)	$C^{g+\Sigma_\pi}$ ($\mu\mathrm{g\,m^{-3}}$)	eff. C^{sat}_{dry} ($\mu\mathrm{g\,m^{-3}}$)
C107OOH	O=CCC1CC(OO)(C(=O)C)C1(C)C	hydroperoxideSOA	0.40	1.60	200.17	8.7918E+00	5.7429E+03
C97OOH	OCC1CC(OO)(C(=O)C)C1(C)C	hydroperoxideSOA	0.44	1.78	188.17	3.9840E+00	3.2741E+02
C108OOH	O=CCC(CC(=O)C(=O)C)C(C)(C)OO	hydroperoxideSOA	0.50	1.60	216.13	1.1344E+00	1.6671E+02

Continuation of Table S5							
MCM Name	SMILES	BAT functionality	O : C	H : C	M_{org} ($\mathrm{g\,mol^{-1}}$)	$C^{g+\Sigma_\pi}$ ($\mu\mathrm{g\,m^{-3}}$)	eff. C^{sat}_{dry} ($\mu\mathrm{g\,m^{-3}}$)
PINIC	OC(=O)CC1CC(C(=O)C)C1(C)C	carboxyl	0.44	1.56	186.17	6.2815E-01	1.4953E+01
C921OOH	OCC(=O)C1(OO)CC(CO)C1(C)C	hydroperoxideSOA	0.56	1.78	204.18	9.1858E-01	2.1280E+00
C812OOH	OCC1CC(OO)(C(=O)O)C1(C)C	hydroperoxideSOA	0.86	1.75	195.17	7.6636E-01	7.1911E-01
C811OH	OCC1CC(C(=O)O)C1(C)C	hydroperoxideSOA	0.38	1.75	158.17	3.9949E-01	1.1569E+03
C813OOH	OCC(CC(=O)C(=O)O)C(C)(C)OO	hydroperoxideSOA	0.75	1.75	206.14	3.1319E-01	3.0180E-02
ALDOL-dimer	CC(=O)C(=O)CC(C(C=O)=CCC1CC(C(O)=O)C1(C)C)C(C)(C)OO	hydroperoxideSOA	0.37	1.47	368.30	4.0696E+00	2.7866E-06
ESTER-dimer	CC1(C)C(CC1C(O)=O)CC(=O)OCC(=O)C2CC(CC(O)=O)C2(C)C	ester	0.37	1.56	368.31	1.0174E+00	3.6370E-06
End of Table							

Table S6: Properties of the isoprene SOA organic mixture used.

Start of Table S6							
MCM Name	SMILES	BAT functionality	O : C	H : C	M_{org} ($\mathrm{g\,mol^{-1}}$)	$C^{g+\Sigma_\pi}$ ($\mu\mathrm{g\,m^{-3}}$)	eff. C^{sat}_{dry} ($\mu\mathrm{g\,m^{-3}}$)
IEB1OOH	OCC(O)C(C)(OO)C=O	hydroperoxideSOA	1.00	2.00	150.11	3.2124E+00	5.0688E+01
IEB2OOH	OOC(C=O)C(C)(O)CO	hydroperoxideSOA	1.00	2.40	150.11	2.4919E-01	2.3180E+02
C59OOH	OCC(=O)C(C)(CO)OO	hydroperoxideSOA	1.00	2.00	150.09	4.2176E+00	2.2954E+01

Continuation of Table S6							
MCM Name	SMILES	BAT functionality	O : C	H : C	M_{org} ($\mathrm{g\,mol^{-1}}$)	$C^{g+\Sigma_\pi}$ ($\mu\mathrm{g\,m^{-3}}$)	eff. C^{sat}_{dry} ($\mu\mathrm{g\,m^{-3}}$)
IEC1OOH	OCC(=O)C(C)(CO)OO	hydroperoxideSOA	1.00	2.00	150.09	1.4709E+00	2.2954E+01
C58OOH	O=CC(O)C(C)(CO)OO	hydroperoxideSOA	1.00	2.00	150.11	3.3475E-01	5.0688E+01
IEPOXA	CC(O)(CO)C1CO1	hydroxyl	0.60	2.00	118.13	8.6354E-11	3.5120E+13
C57OOH	OCC(O)C(C)(OO)C=O	hydroperoxideSOA	1.00	2.00	150.11	2.7170E-01	5.0688E+01
IEPOXC	CC1(CO1)C(O)CO	hydroxyl	0.60	2.00	118.13	2.7879E-09	5.2036E+04
HIEB1OOH	OCC(O)C(CO)(OO)C=O	hydroperoxideSOA	1.20	2.00	166.11	2.8903E-01	1.0370E-01
INDOOH	OCC(ON(=O)=O)C(C)(CO)OO	hydroperoxideSOA	1.40	2.20	197.14	2.5037E-01	4.5117E-01
IEACO3H	CC(O)(C1CO1)C(=O)OO	hydroperoxideSOA	1.00	1.60	148.10	5.3463E-08	5.6321E+04
C525OOH	OCC(=O)C(CO)(CO)OO	hydroperoxideSOA	1.20	2.00	166.09	2.1592E-01	3.9838E-02
HIEB2OOH	OOC(C=O)C(O)(CO)CO	hydroperoxideSOA	1.20	2.00	166.11	1.4203E-01	7.0484E-01
IEC2OOH	OCC(=O)C(C)(OO)C=O	hydroperoxideSOA	1.00	1.60	148.06	2.0876E-06	4.2944E+03
INAOOH	OCC(C)(OO)C(O)CON(=O)=O	hydroperoxideSOA	1.40	2.20	197.14	1.3898E-01	1.7351E+00
C510OOH	O=CC(O)C(C)(OO)CON(=O)=O	hydroperoxideSOA	1.40	1.8	195.10	4.1752E-03	2.6990E+02
INB1OOH	OCC(OO)C(C)(CO)ON(=O)=O	hydroperoxideSOA	1.40	2.20	197.14	7.1561E-02	4.2126E-01
IECCO3H	CC1(CO1)C(O)C(=O)OO	hydroperoxideSOA	1.00	1.60	148.11	7.5983E-07	1.8033E+04

Continuation of Table S6							
MCM Name	SMILES	BAT functionality	O : C	H : C	M_{org} ($\mathrm{g\,mol^{-1}}$)	$C^{g+\Sigma_\pi}$ ($\mu\mathrm{g\,m^{-3}}$)	eff. C^{sat}_{dry} ($\mu\mathrm{g\,m^{-3}}$)
INCOOH	OCC(OO)C(C)(O)CON(=O)=O	hydroperoxideSOA	1.40	2.20	197.14	3.0754E-02	7.3141E+00
INB2OOH	OOCC(O)C(C)(CO)ON(=O)=O	hydroperoxideSOA	1.40	2.20	197.14	3.4893E-02	1.4651E+00
2-Methyltetrol-dimer	CC(O)(CO)C(O)COC(C)(CO)C(O)CO	hydroxyl	0.70	2.30	254.28	7.2215E+00	2.5788E-06
End of Table							

References

Chen, Q., Liu, Y., Donahue, N. M., Shilling, J. E., and Martin, S. T.: Particle-phase chemistry of secondary organic material: Modeled compared to measured O:C and H:C Elemental ratios provide constraints, Environ. Sci. Technol., 45, 4763–4770, https://doi.org/10.1021/es104398s, 2011.

Girolami, G. S.: A Simple "Back of the Envelope" Method for Estimating the Densities and Molecular Volumes of Liquids and Solids, J. Chem. Educ., 71, 962–964, https://doi.org/10.1021/ed071p962, 1994.

Zuend, A. and Seinfeld, J. H.: Modeling the gas-particle partitioning of secondary organic aerosol: The importance of liquid-liquid phase separation, Atmos. Chem. Phys., 12, 3857–3882, https://doi.org/10.5194/acp-12-3857-2012, 2012.